Sustainability in Environment
ISSN 2470-637X (Print) ISSN 2470-6388 (Online)
Vol. 11, No. 2, 2026
www.scholink.org/ojs/index.php/se

Original Paper

Impact of Microplastics on Sulfate Formation via Different Oxidation Pathways

Xuexue Bai[1]

[1] Nanjing University of Information Science and Technology, Nanjing ,China

Received: February 01, 2026 Accepted: March 22, 2026 Online Published: April 10, 2026
doi:10.22158/se.v12n1p203 URL: http://dx.doi.org/10.22158/se.v12n1p203

Abstract

In this paper, the effects of microplastics on sulfate formation under different oxidation paths in atmospheric media were studied. Based on two typical oxidation pathways of hydrogen peroxide (H_2O_2) and ozone (O_3), the regulation of microplastics on sulfate formation mechanism was investigated. The effects of pH value, microplastic dosage and the ratio of S (IV) to oxidant on the promotion of sulfate formation by microplastics were analyzed. The promotion mechanism was discussed by measuring the active species such as hydroxyl radical (•OH) and superoxide radical ($\bullet O_2^-$), combined with material characterization methods. The results showed that both polyvinyl chloride (PVC) and polystyrene (PS) could promote the formation of sulfate in different degrees under the oxidation conditions of H_2O_2 and O_3, and showed different rules under the influence of the above factors. Both of them can promote the decomposition of H_2O_2 and O_3 to generate free radicals, and the formation mechanism of sulfate is driven by adsorption and free radical reaction. In terms of adsorption characteristics, PVC is more likely to adsorb S (VI), while PS shows a stronger adsorption tendency for S (IV).

Keywords

microplastics, sulfate, oxidation mechanism, free radicals

1. Introduction

During severe haze events, atmospheric sulfur dioxide (SO_2) concentration increases significantly, mainly originating from fossil fuel combustion. Liu et al. (2017). Studies indicate that approximately half of SO_2 is converted into sulfate. Adams et al. (2005). Sulfate formation mainly includes gas-phase and aqueous-phase processes. In the gas-phase reaction, SO_2 reacts with hydroxyl radicals (•OH) to form sulfuric acid (H_2SO_4), which is a critical pathway. Calvert et al. (1983). The produced gaseous H_2SO_4 adheres to pre-existing aerosol surfaces or forms new particles under high relative humidity, thereby increasing aerosol concentration and cloud condensation nuclei (CCN) number, further influencing direct and indirect radiative effects. In the aqueous phase, SO_2 dissolves in droplets to form S(IV) (including $SO_2•H_2O$, HSO_3^-, and SO_3^{2-}), which is subsequently oxidized by soluble oxidants such as hydrogen peroxide (H_2O_2), ozone (O_3), oxygen (O_2) catalyzed by transition metal ions (TMIs), and nitrogen dioxide (NO_2) to form sulfate aerosols. Shen et al. (2014). Among these, H_2O is an important oxidant for $SO_2^-$to-SO_4^{2-} conversion due to its high solubility in cloud droplets. In contrast, O_3 solubility is about 17 orders of magnitude lower than that of H_2O_2, leading to a much lower concentration in fog droplets. Seinfeld et al. (1998).

Solution pH significantly affects the aqueous-phase conversion of SO_2 to sulfate. Under atmospheric conditions, at pH 4.5-5.0, the reaction rate of S(IV) with O_2 is considerably lower than that with H_2O_2, so the contribution of the O_2 pathway to sulfate formation can be neglected. Cheng Y et al. (2012). However, recent studies suggest that this reaction mechanism may be severely underestimated in environments with heavy haze and dust pollution . Chameides et al. (1992). Under acidic conditions (pH <5-5.3), the reaction between S(IV) and H_2O_2 is the dominant sulfate formation mechanism (Peeling & Clark, 1983); at higher pH (5-5.3), sulfate is mainly produced via the reaction of S(IV) with O_3.

2. Research design

2.1 Screening of PVC (Polyvinyl Chloride) and PS (Polystyrene)

A total of 40 mL of ultrapure water was first sonicated for 30 minutes, and then purged with argon gas at a flow rate of 40 $mL\cdot min^{-1}$ for 30 minutes to eliminate the interference of dissolved oxygen on the experiment. Subsequently, 80 mg of Na_2SO_3 was added and slowly stirred until completely dissolved. Under airtight conditions, the solution pH was rapidly adjusted to 5 with NaOH/HCl. After adding 160 μL of H_2O_2 with a concentration of 9.79×10^{-2} $mol\cdot L^{-1}$, 5 mg of different microplastics (PVC, PS, PET, PE) were added separately, and the mixture was slowly stirred to form a stable suspension. Samples were collected at 0, 30 s, 1 min, 2 min, 5 min, and 10 min. After filtration through a 0.22 μm aqueous membrane filter, appropriate amounts of 0.1 $mol\cdot L^{-1}$ $BaCl_2$ and HCl were sequentially added to the samples, and the mixture was allowed to stand to generate BaSO4 precipitates. The precipitates were separated by vacuum filtration with a 0.22 μm aqueous membrane filter. The obtained $BaSO_4$ was then calcined in a muffle furnace at 1123 K for 2 hours, cooled, and weighed to record the data. The effects of the four microplastics on sulfate formation via the H_2O_2 oxidation pathway were expressed by the Enhancement Factor (EF):

$$EF=\frac{mBaSO_{4microplastics}-mBaSO_{4(H_2O_2)}}{mBaSO_4} \tag{1}$$

EF(PE) = 0.30, EF(PET) = 0.46, EF(PS) = 0.43, and EF(PVC) = 0.75. A comparison of the enhancement efficiencies of the four microplastics under the H_2O_2 oxidation pathway showed that PVC exhibited the strongest catalytic effect, followed by PET and PS, while PE showed the weakest effect. Therefore, PVC and PS were selected as the main research objects for subsequent experiments.

2.2 Experimental Methods

(1) H_2O_2 Oxidation Pathway

40 mL of terephthalic acid (PTA) solution (10^{-6} mol·L^{-1}) was added into a beaker, followed by the addition of two types of microplastics (PVC and PS), respectively. Samples were taken as blanks, and then 160 μL of 7.5% H_2O_2 was added. Samples were collected at 1 min, 2 min, and 5 min, and measured using a molecular fluorescence spectrometer at an excitation wavelength of 315 nm and an emission wavelength of 335 nm.

(2) O_3 Oxidation Pathway

40 mL of terephthalic acid (PTA) solution with a concentration of 10-6 mol·L-1 was added into a beaker, followed by the addition of polystyrene (PS) and polyvinyl chloride (PVC) microplastic samples, respectively. The mixture without ozone aeration was first collected as the blank control. Subsequently, O_3 was continuously bubbled into the solution at a flow rate of 50 mL·min-1, and samples were taken at 1 min, 2 min, and 5 min. All samples were analyzed using a molecular fluorescence spectrometer with an excitation wavelength of 315 nm and an emission wavelength of 335 nm, and the corresponding fluorescence intensity data were recorded.

(3) Determination of Free Radicals

Hydroxyl Radical (•OH)

40 mL of terephthalic acid (PTA) solution (10-6 mol·L^{-1}) was added into a beaker, followed by the addition of two types of microplastics (PVC and PS), respectively. Samples were collected as blank controls, and then 160 μL of 7.5% H_2O_2 was added. Samples were taken at 1, 2, and 5 min, and detected by a molecular fluorescence spectrometer at an excitation wavelength of 315 nm and an emission wavelength of 335 nm.

Superoxide Radical ($•O_2^-$)

40 mL of nitrotetrazolium blue chloride (NBT) solution (10^{-6} mol·L^{-1}) was added into a beaker, followed by the addition of polystyrene (PS) and polyvinyl chloride (PVC) microplastics, respectively. After collecting the initial sample as a blank control, 160 μL of H_2O_2 solution (9.79×10^{-2} mol·L^{-1}) was added, and samples were collected at 0 s, 30 s, 120 s, and 160 s. The samples were finally measured by a UV-Vis spectrophotometer at a wavelength of 290 nm.

X-ray Photoelectron Spectroscopy (XPS)

To analyze the changes in surface elemental composition and chemical states of microplastics before and after sulfate adsorption, the samples were vacuum-dried at 333 K, and then tested using an ESCALAB 250Xi X-ray photoelectron spectrometer equipped with a monochromatic Al Kα radiation source. The obtained data were processed and analyzed for peak fitting using XPS Peak software.

3. Results and Discussion

3.1 Effects of PVC and PS on Sulfate Formation via H_2O_2 and O_3 Oxidation Pathways under Different Conditions

The pH of aerosol water is a key factor affecting the sulfate formation rate within aerosols. This is because H_2O_2 exhibits strong oxidizing capacity under acidic conditions but weak oxidizing capacity under alkaline conditions, resulting in a significant trend of sulfate formation rate with changing pH. However, in the real atmospheric environment, aerosols exist in various states including steady and unsteady states, leading to uneven pH distribution and further increasing the complexity of this process. Rood et al. (1989).

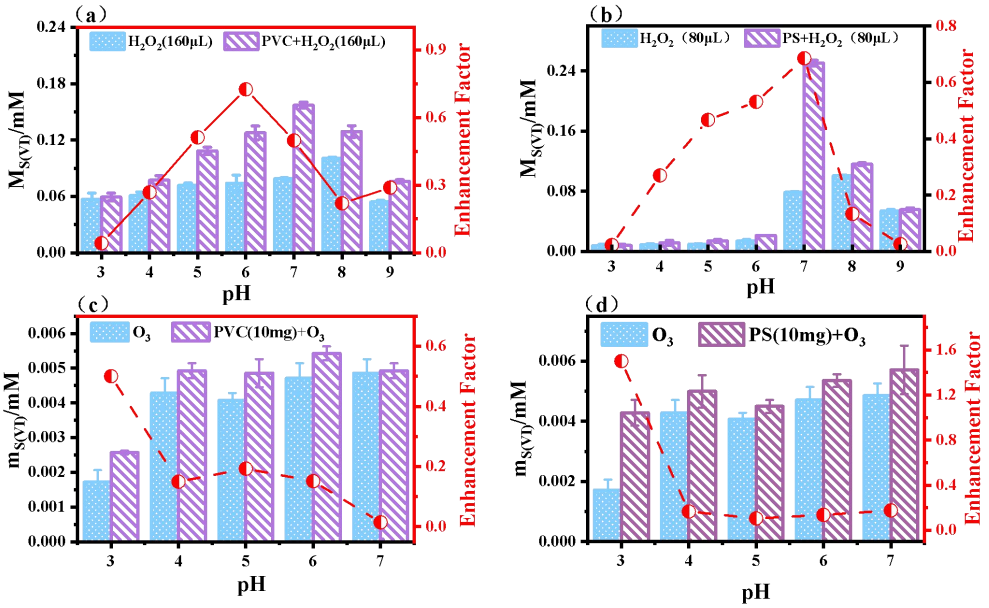

Figure 1. Under different pH Conditions of the Reaction Solution, the Effects of (a) PVC and (b) PS in the H_2O_2 Oxidation Pathway, and (c) PVC and (d) PS in the O_3 Oxidation Pathway on Sulfate Formation

In the H_2O_2 oxidation pathway, the effects of PVC and PS on the sulfate formation rate show distinct pH-dependent patterns (Figure. 1a, b). The difference is that at pH 3-7, the promotion efficiency of PS on sulfate production increases with rising pH, whereas under alkaline conditions, it decreases with further increasing pH (Figure 1b). In the O_3 oxidation pathway, the experimental results of PS at different pH values are generally consistent with those of PVC. However, unlike PVC, the promotion efficiency of PS on sulfate formation at pH 3 is significantly higher than that of PVC under O_3 oxidation. This suggests that microplastics may enhance sulfate yield by promoting O_3 decomposition to generate new reactive species. Nevertheless, this process is strongly influenced by pH, and its promoting effect is relatively limited compared with the oxidation of O_3 itself, thus leading to a different pH-dependent trend.

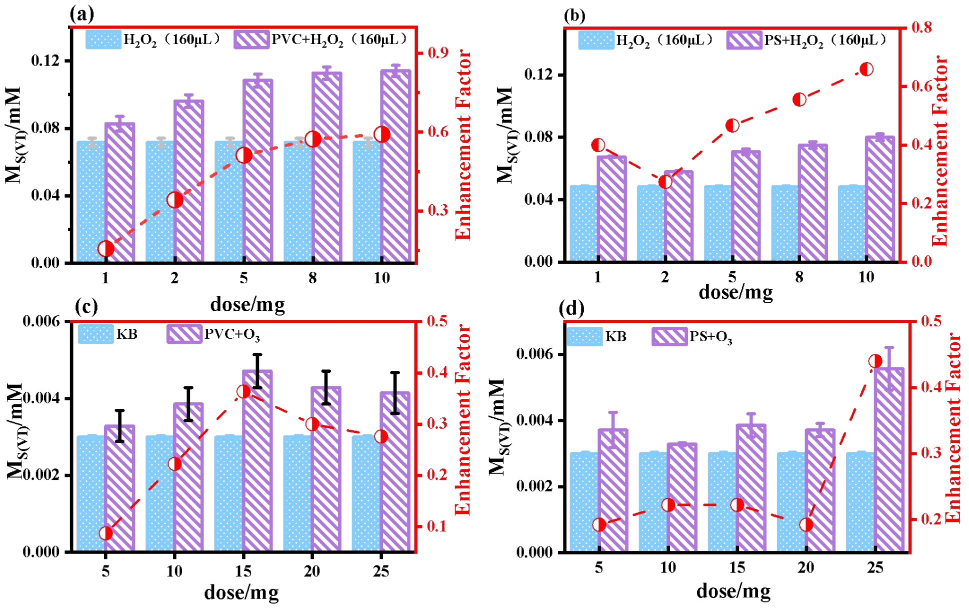

Figure 2. Under Different Dosage Conditions, the Effects of (a) PVC and (b) PS on Sulfate Formation in the H_2O_2 Oxidation Pathway; and the Effects of (c) PVC and (d) PS on Sulfate Formation in the O_3 Oxidation Pathway

With constant dosages of H_2O_2 and sodium sulfite, the enhancement factors (EF) of PVC and PS for sulfate formation exhibited an upward trend with increasing microplastic loading (Figure. 2a, b). This was mainly attributed to the larger contact area between microplastics and dissolved O_3 in solution at higher microplastic concentrations, which favored the generation of more radicals. Meanwhile, the adsorption effect of microplastics also contributed to the enhancement efficiency. However, experimental results showed that the enhancement efficiency decreased slightly when the PVC dosage exceeded 15 mg Figure. 2c, d).

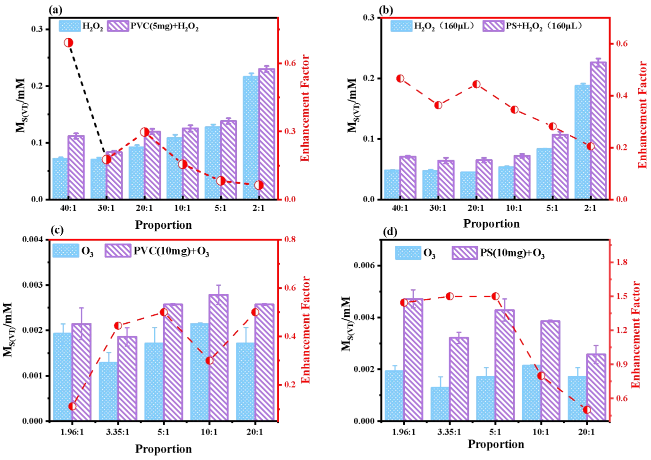

Figure 3. Effects of (a) PVC and (b) PS on Sulfate Formation in the H_2O_2 Oxidation Pathway under different H_2SO_3:H_2O_2/O_3 ratios; and Effects of (c) PVC and (d) PS on Sulfate Formation in the O_3 Oxidation Pathway

Under the condition of H_2O_2 alone (Fig. 3a, b), with a fixed content of Na_2SO_4, the sulfate yield increased after adding PVC or PS compared with the blank group, but its enhancement efficiency decreased continuously with increasing oxidant ratio. According to gas–liquid mass transfer theory, a higher O_3 concentration favors its transfer from the gas phase to the liquid phase, thereby increasing the dissolved O_3 content in the liquid and further promoting sulfate formation. Since PVC can promote O_3 decomposition to generate radicals, the sulfate yield under its action is higher than that in the system with only O_3.

Therefore, in the O_3 oxidation pathway, the enhancement efficiencies of PVC and PS for sulfate formation generally increased with increasing O_3 ratio (Figure. 3c, d). Compared with other microplastics, the benzene-ring structure in PS is easily attacked by O_3. Peeling (1983)[9], forming C-O and O-H groups via oxidation Yang et al (2018)[10]. This process consumes a portion of O_3 and PS, reducing the total amount of O_3 and radicals available for sulfate oxidation. As the O_3 ratio continues to rise, the consumption of PS by the reaction intensifies, causing its enhancement efficiency to decline after an overall increase, showing a trend of slow initial rise followed by a decrease.

3.2 Formation Mechanism of Promoted Sulfate

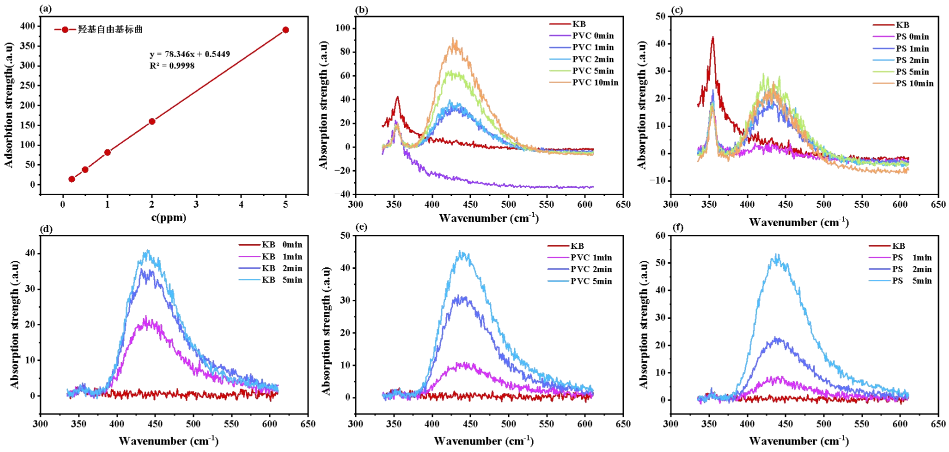

Figure 4. Temporal Variation of •OH Generated by Microplastics-promoted H_2O_2: (a) Standard Curve, (b) PVC, (c) PS; and Temporal Variation of Hydroxyl radicals (•OH) Generated by O_3: (d) Blank Control, (e) PVC, (f) PS

The blank group contained only H_2O_2 (Figure. 4b, c), and the results showed that it could not decompose spontaneously to produce •OH. However, after the addition of PVC or PS, microplastics significantly promoted the decomposition of H_2O_2 to generate •OH, as shown in reactions (1-1), (1-2), (1-3), and (1-4) Kroll et al (2018)[11]:

$$H_2O_2 \rightarrow 2 \bullet OH \tag{2}$$

$$SO_2 + \bullet OH \rightarrow HOSO_2 \tag{3}$$

$$HOSO_2^{-} + O_3 \rightarrow SO_3 + HO_2 \tag{4}$$

$$SO_3+H_2O \rightarrow H_2SO_4 \qquad (5)$$

The high promotion efficiency of PVC for sulfate formation in the H_2O_2 oxidation pathway mainly stems from its ability to continuously catalyze the decomposition of H_2O_2 to produce hydroxyl radicals (•OH). In contrast, PS shows a weaker promoting effect in this pathway because it only induces the generation of a small amount of radicals within a short time. In the O_3 oxidation system, the addition of both PVC and PS can further promote the decomposition of O_3 to form •OH, and the yield of •OH increases with prolonged reaction time. The promoting effect of PS on O_3 decomposition is stronger than that of PVC, which explains why PS exhibits a higher enhancement efficiency for sulfate formation in the O_3 oxidation pathway.

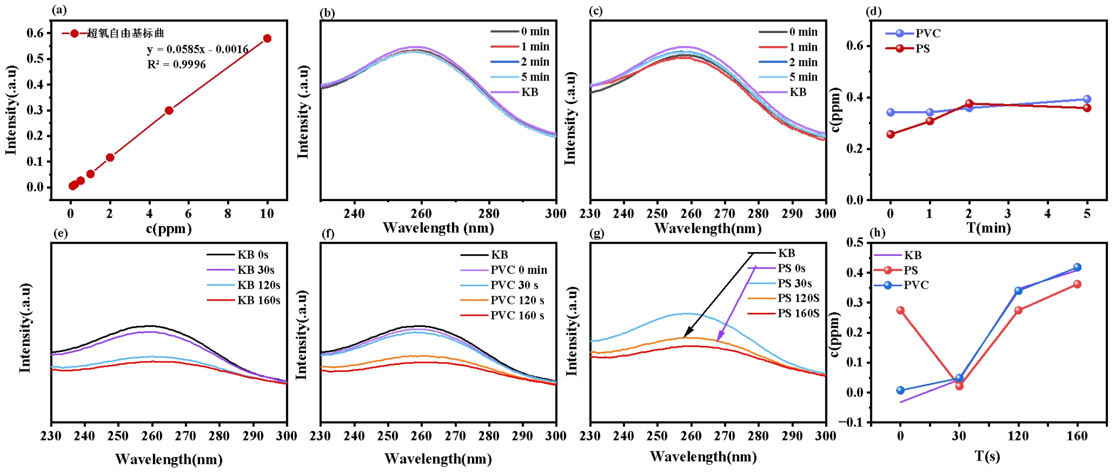

Figure 5. Temporal Variation of Superoxide Radicals (•O_2^-) Generated via the Microplastic-promoted H_2O_2 Oxidation Pathway:(b) PVC, (c)PS, and(d) Concentration Versus Time Plot. Temporal Variation of Superoxide Radicals (•O_2^-) Generated Via the O_3 Oxidation Pathway: (e) Blank Control, (f) PVC, (g) PS, and (h) Concentration Versus Time Plot

In the blank experiment, only the same concentration of H_2O_2 was added, and the results showed that H_2O_2 itself did not decompose to produce superoxide radicals (•O_2^-).However, after the addition of PVC or PS, microplastics significantly promoted the decomposition of H_2O_2 to generate •O_2^-.The reaction equations for •O_2^- are shown in (1-5), (1-6), and (1-7) Kroll et al. (2018):

$$OH+H_2O_2 \rightarrow \bullet HO_2+H_2O \qquad (6)$$

$$HO_2 \rightarrow \bullet O_2^-+H^+ \qquad (7)$$

$$SO_2+\bullet O_2^- \rightarrow O_2SOO^- \qquad (8)$$

After the addition of PVC or PS to the H_2O_2 system, the generation of •O_2^- showed no obvious time dependence. At the initial stage of microplastic addition, the •O_2^- concentration increased rapidly to a relatively high level and then rose only slightly over time (Figure 5d). This indicates that PVC and PS significantly promoted the decomposition of H_2O_2 to produce •O_2^- only within a short period, after which the •O_2^- concentration tended to be stable.In the control experiment with only the same concentration of O_3 added (Figure 5g), O_3 itself was found to decompose to generate •O_2^-. The addition of PVC or PS further accelerated the •O_2^- production from O_3 decomposition (Figures 5e and 5f). After subtracting the background contribution of O_3 (Figure 5h), it can be seen that PVC and PS continuously catalyze the decomposition of O_3 to produce •O_2^-, with the yield increasing over time, thereby continuously promoting the formation of sulfate.

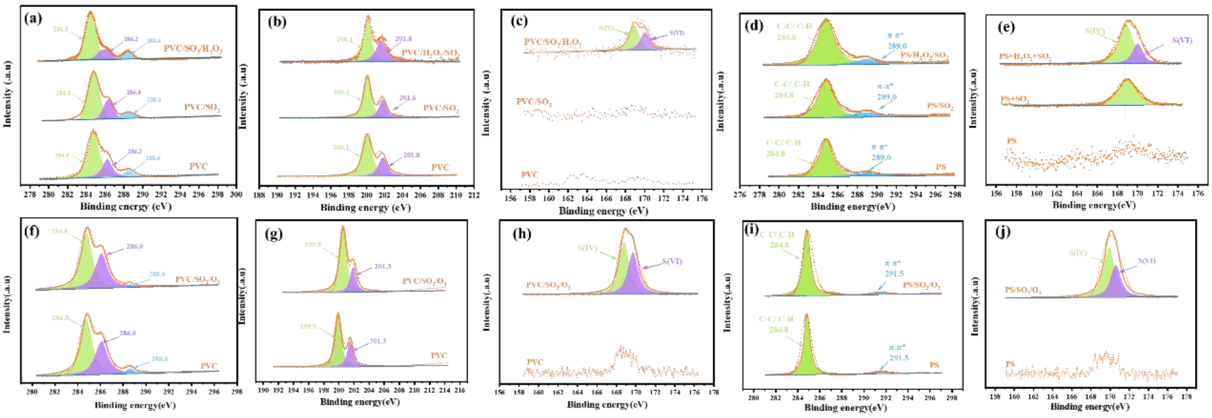

Figure 6. XPS Spectra of Different Elements on the Surface of PVC and PS Materials before and after the Reaction: under the H_2O_2 Oxidation Pathway (a) C, (b) Cl, (c) S for PVC; (d) C, (e) S for PS; under the O_3 Oxidation Pathway (f) C, (g) Cl, (h) S for PVC; (i) C, (j) S for PS

Under the condition of H_2O_2 oxidation, no sulfur signal peak was detected on the surface of the original PVC (Figure.6a), and there was still no sulfur signal after reaction with SO_2. After adding H_2O_2, the characteristic peaks of S (IV) and S (VI) appeared on the surface of PVC (Figure.6c), indicating that SO_2 was dissolved in water to generate SO_3^{2-}, which was oxidized to SO_4^{2-} by free radicals catalyzed by H_2O_2 and PVC in the solution, and finally adsorbed by PVC. Further support this process. The mechanism of PS forming sulfate is consistent with that of PVC (Figure.6d, e).

Existing studies have pointed out that aqueous chlorine radicals (aq $Cl^•$ and aq $Cl_2^{•-}$) are also highly active oxidants Lei et al. (2019), which can be directly or indirectly generated in environmental water bodies Nadtochenko et al. (1998). It has been reported that aq$Cl^•$ can be produced indirectly by the reaction of hydroxyl radical (•OH) with chloride (Cl^-) De et al. (2006). In the mixed system containing PVC, H_2O_2 and S (IV), PVC not only promotes the decomposition of H_2O_2 to generate •OH and •O_2^- , but also the Cl atoms in its structure can react with •OH to generate aqueous chlorine radicals, thereby further improving the yield of sulfate. This mechanism may explain that in a variety of microplastics, PVC has a particularly significant effect on sulfate generation under the H_2O_2 oxidation path.

In contrast, the adsorption capacity of PS to S (IV) is much higher than that of S (VI). This may be because S (IV) first occupies a large number of adsorption sites on its surface and is not easy to desorb, resulting in the gradual accumulation of sulfate on the surface and the decrease of surface activity.

In the O_3 oxidation path, after adding PVC or PS, SO_2 dissolved in water to form SO_3^{2-}, which was then oxidized to SO_4^{2-} by free radicals promoted by O_3 and microplastics, and finally adsorbed on the surface of the material. Compared with the H_2O_2 system, although the content of Cl element in the process increased slightly, it did not actually participate in the reaction, which may be the reason why the promotion effect of PVC under the O_3 oxidation path was weak. At the same time, the increase of O element content in this system was significantly higher than that of S element, indicating that more S (VI) (SO_4^{2-}) was generated, which also explained that the promotion efficiency of PS on sulfate formation was higher than that of PVC under O_3 oxidation conditions.

4. Conclusion

In this paper, the effects of microplastics (PVC, PS) on sulfate formation in different oxidation pathways (H_2O_2 and O_3) were discussed. Under the condition of H_2O_2 oxidation, the adsorption capacity of PVC to S (VI) was significantly stronger than that of S (IV), while the adsorption of PS to S (IV) was more prominent. There are two main reasons why PVC is superior to PS in promoting sulfate formation in H_2O_2 system. First, although both of them can catalyze the decomposition of H_2O_2 to produce reactive oxygen species (•OH and $•O_2^-$), PVC can promote the continuous production of •OH in the system, and PS only induces a small amount of •OH in the short term. Second, the Cl-released from PVC during H_2O_2 oxidation can react with •OH to form an aqueous chlorine radical (aqCl$^•$), which further enhances the formation of sulfate. In the O_3 oxidation pathway, the promotion efficiency of PVC and PS on sulfate formation was regulated by many factors such as pH, dosage and the ratio of reducing agent to oxidant. The study of the two oxidation pathways shows that PVC and PS have different advantages in different systems : under the H_2O_2 oxidation pathway, PVC promotes the formation of sulfate more significantly ; under O_3 oxidation conditions, PS showed higher promotion efficiency.

Acknowledgments

This paper was supported by Project supported by National Natural Science Foundation of China (42473024)

References

Adams, J. W., Rodriguez, D., & Cox, R. A. (2005). The uptake of SO_2 on Saharan dust: A flow tube study. *Atmospheric Chemistry and Physics*, *5*(10), 2679-2689.

Calvert, J. G., & Stockwell, W. R. (1983). Acid generation in the troposphere by gas-phase chemistry. *Environmental science & technology*, *17*(9), 428A-443A.

Chameides, W. L., & Stelson, A. W. (1992). Aqueous-phase chemical processes in deliquescent sea-salt aerosols: A mechanism that couples the atmospheric cycles of S and sea salt. *Journal of Geophysical Research: Atmospheres*, *97*(D18), 20565-20580.

Cheng, Y., Zheng, G., Wei, C. et al. (2016). Reactive nitrogen chemistry in aerosol water as a source of sulfate during haze events in China. *Science advances*, *2*(12), e1601530.

De Laat, J., & Le, T. G. (2006). Effects of chloride ions on the iron (III)-catalyzed decomposition of hydrogen peroxide and on the efficiency of the Fenton-like oxidation process. *Applied Catalysis B: Environmental*, *66*(1-2), 137-146.

Kroll, J. A., Frandsen, B. N., Kjaergaard, H. G. et al. (2018). Atmospheric hydroxyl radical source: Reaction of triplet SO2 and water. *The Journal of Physical Chemistry A*, *122*(18), 4465-4469.

Lei, Y., Cheng, S., Luo, N. et al. (2019). Rate constants and mechanisms of the reactions of $\mathrm{Cl}^{\bullet}$ and $\mathrm{Cl}_2^{\bullet-}$ with trace organic contaminants. *Environmental science & technology*, *53*(19), 11170-11182.

Liu, M., Song, Y., Zhou, T. et al. (2017). Fine particle pH during severe haze episodes in northern China. *Geophysical Research Letters*, *44*(10), 5213-5221.

Nadtochenko, V. A., & Kiwi, J. (1998). Photolysis of FeOH^{2+} and FeCl^{2+} in aqueous solution. Photodissociation kinetics and quantum yields. *Inorganic Chemistry*, *37*(20), 5233-5238.

Peeling, J., & Clark, D. T. (1983). Surface ozonation and photooxidation of polyethylene film. *Journal of Polymer Science: Polymer Chemistry Edition*, *21*(7), 2047-2055.

Rood, M. J., Shaw, M. A., Larson, T. V. et al. (1989). Ubiquitous nature of ambient metastable aerosol. *Nature*, *337*(6207), 537-539.

Seinfeld, J. H., & Pandis, S. N. (1998). *Atmospheric chemistry and physics: From air pollution to climate change*. Wiley.

Shen, X., Lee, T., Guo, J. et al. (2012). Aqueous phase sulfate production in clouds in eastern China. *Atmospheric Environment*, *62*, 502-511.

Yang, R., He, Q., Wang, C. et al. (2018). Surface modification of polystyrene microsphere using ozone treatment. *Ferroelectrics*, *530*(1), 130-135.